rocity theorem for the total and incident fields in region S_i yields

$$\oint_{C_i} (E_z\tilde{H}_l - \tilde{E}_z H_l)\, dl = 0, \qquad i = 1,2,\cdots,M \tag{16}$$

and the equation given by substituting the incident fields for the total fields in (16). Considering the radiation condition and the boundary condition (2), the reciprocity theorem for the scattered fields in region S_0 gives the same relation in which C_i is replaced with $C_1 + C_2 + \cdots + C_M$. We have then

$$\sum_{i=1}^{M} \oint_{C_i} [(E_z^{sc}\tilde{H}_l^{inc} - \tilde{E}_z^{inc}H_l^{sc}) - (\tilde{E}_z^{sc}H_l^{inc} - E_z^{inc}\tilde{H}_l^{sc})]\, dl = 0. \tag{17}$$

The integral expression for the scattered fields can be obtained, using the Green's function which vanishes on the reflector. In the radiation zone the scattered field of the direction $\tilde{\theta}$ becomes

$$\begin{aligned} E_z^{sc}|_{\tilde{\theta}} \simeq -\left(\frac{jk_0}{8\pi r}\right)^{1/2} \exp(-jk_0 r) \sum_{i=1}^{M} \oint_{C_i} &\cdot \{[z_0 H_l^{sc} - E_z^{sc}\cos(\psi - \tilde{\theta})] \\ &\cdot \exp[jk_0 r' \cos(\phi' - \tilde{\theta})] \\ &- [z_0 H_l^{sc} - E_z^{sc}\sin(\psi + \tilde{\theta})] \\ &\cdot \exp[jk_0 r' \sin(\phi' + \tilde{\theta})] \\ &+ [z_0 H_l^{sc} + E_z^{sc}\cos(\psi - \tilde{\theta})] \\ &\cdot \exp[-jk_0 r' \cos(\phi' - \tilde{\theta})] \\ &- [z_0 H_l^{sc} + E_z^{sc}\sin(\psi + \tilde{\theta})] \\ &\cdot \exp[-jk_0 r' \sin(\phi' + \tilde{\theta})]\}\, dl' \end{aligned} \tag{18}$$

where ψ is the angle between $\boldsymbol{n}$ and the x axis, and $\boldsymbol{r}' = (r',\phi')$ is a vector on the boundaries of the cylinders. From (18) and (17) accompanied with the expressions for the respective incident fields, the following reciprocity relation of the scattered fields can be derived:

$$E_z^{sc}|_{\tilde{\theta}} = \tilde{E}_z^{sc}|_{\theta}, \qquad \text{in the far zone.} \tag{19}$$

The sum of the scattered power and the power absorbed in the cylinders can be rewritten as

$$\begin{aligned} P^{abs} + P^{sc} &= \tfrac{1}{2}\,\mathrm{Re} \sum_{i=1}^{M} \oint_{C_i} (E_z H_l^* - E_z^{sc}H_l^{sc*})\, dl \\ &= \tfrac{1}{2}\,\mathrm{Re} \sum_{i=1}^{M} \oint_{C_i} (E_z^{inc*}H_l^{sc} + E_z^{sc}H_l^{inc*})\, dl. \end{aligned} \tag{20}$$

From (18), (20), and (10a) we obtain

$$P^{abs} + P^{sc} = -(1/z_0)\,\mathrm{Re}\,[(2\pi r/jk_0)^{1/2} \exp(jk_0 r) E_z^{sc}|_{\theta}] \tag{21}$$

that is, $P^{abs} + P^{sc}$ is related to the scattered field in the direction of the plane-wave source. This relation corresponds to the forward scatter theorem for the case that the reflector is removed [12], however, it should be called "backward scatter theorem" in this case.

Appendix II
Scattering of Waves Generated by Source Near to Obstacles

Consider the arrangements as shown in Fig. 1(a) and the same obstacles composed of transposed media. The reciprocity theorem in the respective regions S_i and S_0 accompanied with the radiation conditions and the boundary condition (2) gives (16) and

$$\sum_{i=1}^{M} \oint_{C_i} (E_z\tilde{H}_l - \tilde{E}_z H_l)\, dl = \int_{S_0} (\tilde{E}_z J_z - E_z \tilde{J}_z)\, dS \tag{22}$$

where magnetic current sources are disregarded. Combination of (16) with (22) yields the reciprocity relation

$$\int_{S_0} \tilde{E}_z J_z\, dS = \int_{S_0} E_z \tilde{J}_z\, dS. \tag{23}$$

The incident fields satisfy a similar relation and so do the scattered fields. If an electric current filament (9a) is considered,

$$\tilde{E}_z^{sc}(\boldsymbol{u}) = E_z^{sc}(\tilde{\boldsymbol{u}}) \tag{24}$$

holds where a current filament $\tilde{J}_z$ is located at $\tilde{\boldsymbol{u}}$.

Acknowledgment

The author is greatly indebted to Prof. R. Yamada for the support of this research. He also wishes to express his thanks to Prof. K. Fujisawa of Osaka University for criticism and encouragement. The numerical calculations were performed on the NEAC 2200-700 at Osaka University.

References

[1] W. H. Eggimann, "Scattering of a plane wave on a ferrite cylinder at normal incidence," *IRE Trans. Microwave Theory Tech.*, vol. MTT-8, pp. 440–445, July 1960.
[2] P. M. Platzmann and H. T. Ozaki, "Scattering of electromagnetic waves from an infinitely long magnetized cylindrical plasma," *J. Appl. Phys.*, vol. 31, pp. 1597–1601, Sept. 1960.
[3] Y. Chow, "Scattering of electromagnetic waves by coaxial ferrite cylinders of different tensor permeabilities," *Appl. Sci. Res. B* (Netherlands), vol. 8, pp. 290–298, 1960.
[4] Y. Ohba, "Diffraction by a conducting circular cylinder clad by an anisotropic plasma sheath," *Can. J. Phys.*, vol. 41, pp. 881–889, June 1963.
[5] H. C. Chen and D. K. Cheng, "Scattering of electromagnetic waves by an anisotropic plasma-coated conducting cylinder," *IEEE Trans. Antennas Propagat.*, vol. AP-12, pp. 348–353, May 1964.
[6] K. Germey, "Die Beugung einer ebenen electromagnetischen Welle an zwei parallelen unendlich langen idealleitenden Zylindern von elliptischen Querschnitt," *Ann. Phys.*, 7 Folge vol. 13, pp. 237–251, 1964.
[7] N. Okamoto, Y. Yoshimura, Y. Nakanishi, and S. Kumagai, "Scattering of a plane electromagnetic wave by two parallel infinitely long ferrimagnetic cylinders," *J. Inst. Elec. Commun. Eng. Jap.*, vol. 49, pp. 2431–2438, Dec. 1966.
[8] P. C. Waterman, "Matrix formulation of electromagnetic scattering," *Proc. IEEE*, vol. 53, pp. 805–812, Aug. 1965.
[9] N. Okamoto, "Matrix formulation of scattering by a homogeneous gyrotropic cylinder," *IEEE Trans. Antennas Propagat.*, vol. AP-18, pp. 642–649, Sept. 1970.
[10] ——, "Scattering by a gyrotropic cylinder coated with another gyrotropic layer," *J. Inst. Electron. Commun. Eng. Jap.*, vol. 55-B, pp. 233–240, May 1972.
[11] ——, "Electromagnetic scattering by many gyrotropic cylinders of different kinds," *IEEE Trans. Antennas Propagat.*, vol. AP-22, pp. 701–707, Sept. 1974.
[12] J. G. Van Bladel, *Electromagnetic Fields.* New York: McGraw-Hill, 1964, pp. 254–258.

An Impedance Sheet Approximation for Thin Dielectric Shells

ROGER F. HARRINGTON AND JOSEPH R. MAUTZ

***Abstract*—An approximate equivalence between an impedance loaded surface and a thin dielectric shell is given. This approximation is used to compute the backscattering from a thin circular dielectric tube and the results are compared to the exact solution. Computations for backscattering from a thin dielectric cone-sphere and resonant wire loop inside of a thin dielectric cylinder are also given as further illustrations of the method.**

Manuscript received September 10, 1974; revised January 6, 1975.
The authors are with the Department of Electrical and Computer Engineering, Syracuse University, Syracuse, N.Y. 13210.

I. Introduction

For aerodynamic reasons an antenna or scatterer is sometimes enclosed in a thin dielectric shell. Analyses and computer programs exist for calculating the electromagnetic behavior of an impedance loaded surface [1]–[3]. These existing programs can be used to calculate the behavior of a thin dielectric shell if it is represented as an impedance load. This paper describes an approximate equality between a dielectric shell and an impedance sheet, and uses it for some representative computations. The approximation is valid for lossy dielectrics as well as loss-free dielectrics. In the lossy case the impedance sheet has both a real and imaginary part, while for the loss-free case it is purely reactive. Similar approximations have been used by others for thin dielectric spherical shells [4] and for thin plasma sheets [5], [6].

II. Basic Theory

The operator formulation for scattering by a dielectric body is available in the literature [7], [8]. Consider a body of volume V with dielectric constant ε in an impressed field $\boldsymbol{E}^i$. The polarization current $\boldsymbol{J}$ is then given by

$$L(\boldsymbol{J}) + \frac{\boldsymbol{J}}{j\omega(\varepsilon - \varepsilon_0)} = \boldsymbol{E}^i, \qquad \text{in } V \tag{1}$$

where the operator L is that which relates the scattered field $\boldsymbol{E}^s$ to the polarization current according to

$$L(\boldsymbol{J}) = -\boldsymbol{E}^s = j\omega \boldsymbol{A} + \nabla\phi. \tag{2}$$

Here $\boldsymbol{A}$ and ϕ are the magnetic vector potential and the electric scalar potential

$$\boldsymbol{A}(\boldsymbol{r}) = \mu_0 \iiint_V \boldsymbol{J}(\boldsymbol{r}') \frac{e^{-jkR}}{4\pi R}\, d\tau' \tag{3}$$

$$\phi(\boldsymbol{r}) = \frac{1}{\varepsilon_0} \iiint_V q(\boldsymbol{r}') \frac{e^{-jkR}}{4\pi R}\, d\tau'. \tag{4}$$

$R = |\boldsymbol{r} - \boldsymbol{r}'|$ is the distance from a source point $\boldsymbol{r}'$ to a field point $\boldsymbol{r}$, and $k = 2\pi/\lambda_0$ is the free-space wavenumber. The charge density is related to the polarization current density by the equation of continuity

$$\nabla \cdot \boldsymbol{J} = -j\omega q. \tag{5}$$

Hence, (1) is an integro-differential equation to determine $\boldsymbol{J}$ when $\boldsymbol{E}^i$ is given.

Suppose (1) is now specialized to a thin dielectric shell of thickness t on a surface S, as suggested by Fig. 1. If the dielectric constant is large, the polarization current will have a large component of $\boldsymbol{J}$ tangential to S. If we neglect the normal component of current, and express the tangential component in terms of the net surface current $\boldsymbol{J}_s$, then (1) can be rewritten as

$$Z(\boldsymbol{J}_s) + \frac{\boldsymbol{J}_s}{j\omega\, \Delta\varepsilon t} = \boldsymbol{E}^i_{\tan}, \qquad \text{on } S. \tag{6}$$

Here $\Delta\varepsilon = \varepsilon - \varepsilon_0$, the subscript "tan" denotes the tangential component on S, and $Z(\boldsymbol{J}_s)$ is the impedance operator

$$Z(\boldsymbol{J}_s) = -\boldsymbol{E}^s_{\tan} = [L(\boldsymbol{J})]_{\tan}. \tag{7}$$

Note that (6) is precisely the equation which applies to a surface S loaded by a reactive sheet

$$Z_L = \frac{1}{j\omega\, \Delta\varepsilon t}. \tag{8}$$

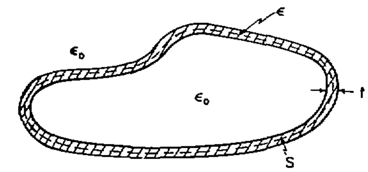

Fig. 1. Thin dielectric shell.

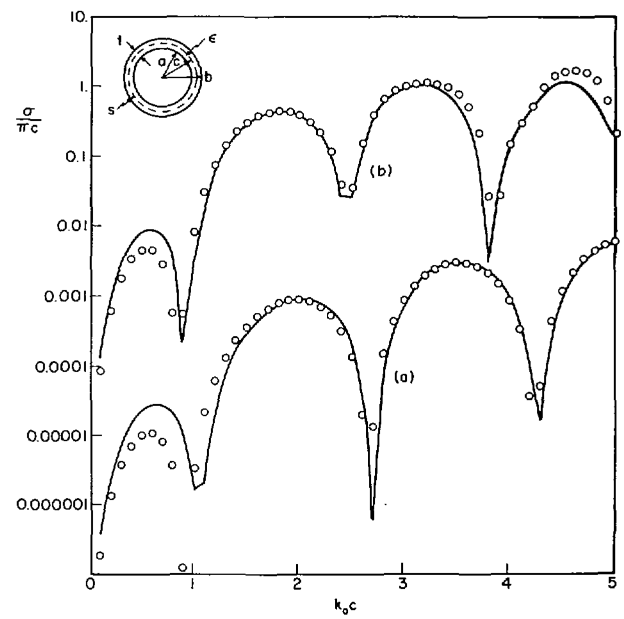

Fig. 2. Normalized backscattering width $\sigma/\pi c$ versus normalized frequency $k_0c = 2\pi c/\lambda_0$ for cylindrical dielectric shell. Exact solution is shown solid, reactance sheet approximation is shown by circles. Curve (a), $\varepsilon = 2.56\varepsilon_0$, $t = 0.01c$. Curve (b), $\varepsilon = 5\varepsilon_0$, $t = 0.1c$.

Impedance loaded surfaces have been studied extensively in previous work [1]–[3]. Hence, if the dielectric shell is approximated by a reactive load according to (8), we can use previously developed computer programs to study the dielectric shell problem. Lossy dielectric shells can be treated by considering ε to be complex in (8).

III. Application to Dielectric Cylinders

To test the validity of the reactance sheet approximation to a dielectric shell the theory was first applied to a thin cylindrical dielectric shell. This is a problem for which the exact solution is known [9]. The geometry is as shown in the insert in Fig. 2. The inner radius of the cylinder is denoted by a and the outer radius by b. Hence, the thickness of the dielectric shell is $t = b - a$ and the average radius is $c = (a + b)/2$. The excitation is a plane wave with $\boldsymbol{E}^i$ perpendicular to the axis of the cylinder (transverse electric excitation). Computations were made for normalized backscattering width $(\sigma/\pi c)$ versus normalized frequency $(k_0c = 2\pi c/\lambda_0)$ for both the exact solution and the reactive sheet approximation. Fig. 2 shows two such computations, curve (a) being for $\varepsilon = 2.56\varepsilon_0$ and $t = 0.01c$, and curve (b) being for $\varepsilon = 5\varepsilon_0$ and $t = 0.1c$. The exact solution (computed at increments of 0.1) is shown solid and the reactive sheet solution by circles. As given by (8), the approximate solution is a function of only $\Delta\varepsilon t$, not of ε and t independently. Note that the approximate solution is close to the exact solution in both cases over the range of k_0c from 0 to 5, the largest discrepancy occurring for small k_0c. It is felt that this is due to the small radius of curvature of the shell with respect to wavelength. The approximation for large $\Delta\varepsilon t$ is better than that for small $\Delta\varepsilon t$. We would

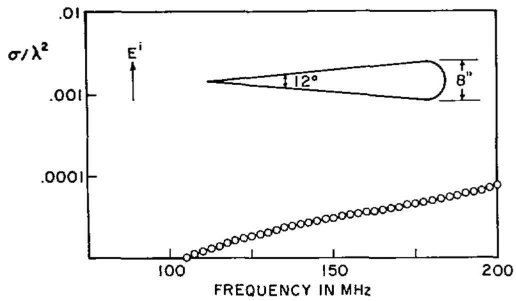

Fig. 3. Normalized backscattering cross section σ/λ^2 versus frequency for thin dielectric cone-sphere. Excitation is plane wave axially incident on tip. $\Delta\varepsilon t = \varepsilon_0 a$, where a is radius of sphere.

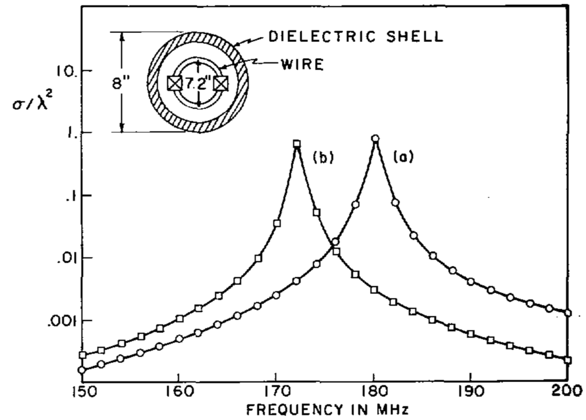

Fig. 4. Normalized backscattering cross section σ/λ^2 versus frequency for resonant loop with and without thin dielectric cylinder surrounding it. Curve (a), no cylinder. Curve (b), $\Delta\varepsilon t = 0.4\varepsilon_0 a$, where a = cylinder radius.

expect the approximations to become exact in the limit as $\varepsilon \to \infty$ and $t \to 0$ such that $\Delta\varepsilon t$ remains finite. Computations for very large $\Delta\varepsilon t$ verify this expectation.

IV. Application to Dielectric Cone-Spheres

The theory is next applied to a dielectric shell in the shape of a cone-sphere, as shown in the insert of Fig. 3. The excitation is a plane wave axially incident on the cone-sphere. When the reactive sheet approximation is used, the body is a special case of an impedance loaded body of revolution for which general computer programs exist [2]. With axial incidence, only the $m = 1$ mode of the body is excited. A reactive load impedance matrix obtained from (8) must be added to the generalized impedance matrix for the body. Since the expansion functions are triangle functions of the contour length variable, the load impedance matrix becomes a tridiagonal reactive matrix. Once this matrix is calculated, the computer programs of [2] can be used to calculate the radar scattering cross section. Computations were made of the normalized backscattering cross section (σ/λ^2) versus frequency (from 100 to 200 MHz) for the dielectric shell cone-sphere. The values of $\Delta\varepsilon t$ used range from $0.01\varepsilon_0 a$ to $1.0\varepsilon_0 a$, corresponding to ε ranging from $2\varepsilon_0$ to $11\varepsilon_0$ and t from $0.1a$ to $0.01a$, where a is the radius of the sphere. For the smaller values of $\Delta\varepsilon t$ the σ/λ^2 was below 10^{-5} over the entire range of frequencies. A plot of σ/λ^2 for the largest value, $\Delta\varepsilon t = \varepsilon_0 a$, is shown in Fig. 3. Even in this case σ/λ^2 was below 10^{-4} over the entire range, being largest at the higher frequencies.

V. Wire Scatterer and Impedance Sheet of Revolution

Consider a body of revolution which has a surface impedance $\mathscr{Z}$, and a wire object which is assumed to be a perfect conductor. The sheet and wire are illuminated by an incident field $\boldsymbol{E}^i$. Let $\boldsymbol{J}^s$ denote the current on the impedance sheet, and $\boldsymbol{J}^w$ the current on the wire. The functional equations to be satisfied are

$$L^{ss}(\boldsymbol{J}^s) + \mathscr{Z}(\boldsymbol{J}^s) + L^{sw}(\boldsymbol{J}^w) = \boldsymbol{E}^i_{\tan} \tag{9}$$

on the impedance sheet, and

$$L^{ws}(\boldsymbol{J}^s) + L^{ww}(\boldsymbol{J}^w) = \boldsymbol{E}^i_{\tan} \tag{10}$$

on the wire. Here L denotes the operator relating $-\boldsymbol{E}$ to $\boldsymbol{J}$, the first superscript denoting the object on which the field is evaluated, and the second superscript denoting the object on which the current exists.

Following the method of moments [8], we define a set $\{\boldsymbol{J}_i^s\}$ of current expansion functions and approximate the current on the impedance sheet by

$$\boldsymbol{J}^s = \sum_i I_i^s \boldsymbol{J}_i^s \tag{11}$$

where I_i^s are coefficients. Similarly, we define a set $\{\boldsymbol{J}_j^w\}$ of current expansion functions and approximate the current on the wire by

$$\boldsymbol{J}^w = \sum_j I_j^w \boldsymbol{J}_j^w \tag{12}$$

where I_j^w are coefficients. It is convenient, but not necessary, to take the $\boldsymbol{J}_i^s$ to be the same expansion functions as used in previous work on bodies of revolution [1], and the $\boldsymbol{J}_j^w$ to be the same as used in previous work on wire objects [10]. For testing functions, we also assume those used in previous work, in which case $\{\boldsymbol{W}_i^s\} = \{\boldsymbol{J}_i^{s*}\}$, and $\{\boldsymbol{W}_j^w\} = \{\boldsymbol{J}_j^w\}$. Now (11) and (12) are substituted into (9) and (10), and the results tested with the appropriate testing functions and inner products. This leads to the matrix equations

$$[Z^{ss} + Z_L]\boldsymbol{I}^s + [Z^{sw}]\boldsymbol{I}^w = \boldsymbol{V}^s \tag{13}$$

and

$$[Z^{ws}]\boldsymbol{I}^s + [Z^{ww}]\boldsymbol{I}^w = \boldsymbol{V}^w. \tag{14}$$

Here the matrices $[Z^{ss}]$ and $[Z^{ww}]$, and the excitation vectors $\boldsymbol{V}^s$ and $\boldsymbol{V}^w$, are the same as used in previous work [2], [10]. The load matrix $[Z_L]$ is the same as that used previously for loaded bodies of revolution [2]. The $\boldsymbol{I}^s$ and $\boldsymbol{I}^w$ are the vectors of the unknown coefficients I_i^s and I_j^w. The only new quantities to be evaluated are the elements of $[Z^{sw}] = [\tilde{Z}^{ws}]$, the interaction matrices. Once all the matrices are evaluated, (13) and (14) can be solved for $\boldsymbol{I}^s$ and $\boldsymbol{I}^w$, and the currents obtained by (11) and (12). The scattered field from these currents is then found in the usual way.

VI. Application to a Loaded Wire Loop in a Short Dielectric Cylinder

The solution of the previous section has been implemented in a computer program for loaded wire objects near a loaded surface of revolution [11]. This program has been tested on a number of simple problems, of which Fig. 4 is typical. The scatterer consists of a circular wire loop with two reactive loads X to resonate it at 180 MHz, surrounded by a thin dielectric cylinder. The diameter of the loop is 7.2 in. and the diameter of the wire is 0.08 in. The diameter of the dielectric cylinder is 8 in. and its length is 8 in. The excitation is a plane wave axially incident on the cylinder and loop, with $\boldsymbol{E}$ polarized vertically. The normalized backscattering cross section σ/λ^2 was computed for the frequency range of 150 to 200 MHz. In Fig. 4 curve (a) is for $\Delta\varepsilon t = 0$, in which case the dielectric cylinder is not present. Curve (b) is for

$\Delta\varepsilon t = 0.4\varepsilon_0 a$, where a = cylinder radius = 0.1016 m. Note that the principal effect of the dielectric cylinder is to shift the resonance to a lower frequency.

VII. Discussion

The impedance sheet approximation for thin dielectric shells has been used to compute the electromagnetic behavior of thin shells using computer programs developed for loaded bodies. Far-field quantities, such as radar cross section and antenna gain patterns, are probably accurate. It is expected that near-field quantities would be less accurate. The method could be extended to include the normal component of polarization current, in which case it would, in principle, be exact. However, this would complicate the solution and require the development of new computer programs.

References

[1] R. F. Harrington and J. R. Mautz, "Radiation and scattering from loaded bodies of revolution," *Appl. Sci. Res.*, vol. 26, pp. 209–217, June 1971.

[2] ——, "Computation of radiation and scattering from loaded bodies of revolution," Sci. Rep. 4, Contract F19628-68-C-0180 with Air Force Cambridge Research Laboratories, AD 701-744, Jan. 1970.

[3] ——, "Control of radar scattering by reactive loading," *IEEE Trans. Antennas Propagat.*, vol. AP-20, pp. 446–454, July 1972.

[4] M. G. Andreasen, "Backscattering cross section of a thin, dielectric, spherical shell," *IRE Trans. Antennas Progapat.*, vol. AP-5, pp. 267–270, July 1957.

[5] J. R. Wait, "Propagation of electromagnetic waves along a thin plasma sheet," *Can. J. Phys.*, vol. 28, no. 12, pp. 1586–1594, Dec. 1960.

[6] R. L. Fante, "Effect of thin plasmas on an aperture antenna in an infinite conducting plane," *Radio Sci.*, vol. 2 (new series), pp. 87–100, Jan. 1967.

[7] J. H. Richmond, "Scattering by a dielectric cylinder of arbitrary cross section shape," *IEEE Trans. Antennas Propagat.*, vol. AP-13, pp. 334–341, May 1965.

[8] R. F. Harrington, *Field Computation by Moment Methods.* New York: Macmillan, 1968.

[9] G. T. Ruck, D. E. Barrick, W. D. Stuart, and C. K. Krichbaum, *Radar Cross Section Handbook*, vol. 1. New York: Plenum, 1970.

[10] D. C. Kuo, H. H. Chao, J. R. Mautz, B. J. Strait, and R. F. Harrington, "Analysis of radiation and scattering by arbitrary configurations of thin wires," *IEEE Trans. Antennas Propagat.* (CPD), vol. AP-20, pp. 814–815, Nov. 1972.

[11] J. R. Mautz, "Scattering from loaded wire objects near a loaded surface of revolution," Syracuse University Research Corporation, Rep. SURC TN 74-030, Jan. 1974.

Analysis of Various Numerical Techniques Applied to Thin-Wire Scatterers

CHALMERS M. BUTLER AND D. R. WILTON

***Abstract*—Several numerical schemes for solving Pocklington's and Hallén's equations for thin-wire scatterers are investigated. Convergence rates of solutions obtained from seven methods are given and reasons for different rates are delineated.**

Introduction

In moment method solutions of antenna and scattering problems associated with thin-wire structures, both Pocklington (electric field) and Hallén (magnetic vector potential) type integral equations are commonly used. From either, one may obtain solutions for the current on a wire antenna or a scatterer and subsequently calculate all other quantities of interest. Even though the two equations are intimately related [1], each exhibits distinct advantages and disadvantages. The authors present the findings of their investigations of several numerical schemes for solving wire problems. They discuss the relative merits of various techniques, point out pitfalls to be avoided, and summarize their findings.

Manuscript received August 1, 1974; revised December 23, 1974. This work was supported in part by the National Science Foundation under Grant GU3833.

The authors are with the School of Engineering, University of Mississippi, University, Miss. 38677.

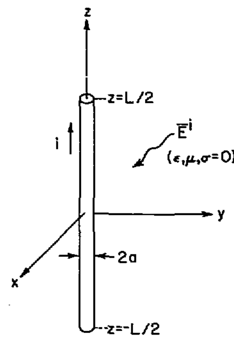

Fig. 1. Straight wire subject to incident illumination.

In the numerical methods, different basis sets for representing the unknown wire current are employed and relative convergences are investigated. So that one may focus attention on the generic feature of the capacity of a given basis set to represent adequately, and converge to, the correct current on the wire, only the case of a scatterer subject to normally incident illumination is considered here. With illumination constant over the length of the scatterer, the problem of inadequate sampling [2] of the integral equation's driving term has no bearing on convergence. Also, in the interest of simplicity and of addressing only the fundamental question of convergence in the sense of how well the actual wire current is represented by the solution, the wire junction problem is not treated nor is any record of computer times given for the various methods.

Thin-Wire Equations

From basic electromagnetic theory, one may readily obtain the following fundamental integro-differential equation:

$$\left(\frac{d^2}{dz^2} + k^2\right) \int_{\zeta=-L/2}^{L/2} i(\zeta) K(z - \zeta)\, d\zeta = -j4\pi\omega\varepsilon E_z^i(z) \quad (1)$$

which relates the unknown total axial current i on a cylinder to the known incident electric field having an axial component E_z^i on the surface of the scatterer. The scatterer is perfectly conducting and resides in a homogeneous space characterized by (μ, ε, $\sigma = 0$), and, as suggested in Fig. 1, it is a tube of length L and radius a. The kernel in (1) is

$$K(\xi) = \frac{1}{2\pi} \int_{\phi'=-\pi}^{\pi} \frac{e^{-jk[\xi^2 + 4a^2 \sin^2(\phi'/2)]^{1/2}}}{[\xi^2 + 4a^2 \sin^2(\phi'/2)]^{1/2}}\, d\phi' \quad (2)$$

where k is 2π/wavelength at the angular frequency ω of the suppressed harmonic time variation $e^{j\omega t}$. For present purposes, the wire radius is looked upon as being very small relative to the wavelength λ as well as to the cylinder length. Such restrictions, common in thin-wire analyses, assure one that the current on the cylinder is circumferentially independent and that it can be accounted for by the total axial current i. The thin-wire assumptions also lead to the so-called reduced kernel approximation to $K(\xi)$

$$K(\xi) \doteq \frac{e^{-jk[\xi^2 + a^2]^{1/2}}}{[\xi^2 + a^2]^{1/2}}. \quad (3)$$